Leadership in Sustainable Infrastructure
Leadership en Infrastructures Durables

Vancouver, Canada
May 31 – June 3, 2017/ *Mai 31 – Juin 3, 2017*

EFFECT OF GEOMETRIC IMPERFECTION AND RESIDUAL STRESS ON THE FINITE ELEMENT MODELLING OF STAINLESS STEEL I-SECTIONS SUBJECTED TO LATERAL-TORSIONAL BUCKLING

Anwar-Us-Saadat, Mohammad[1,4] and Ashraf, Mahmud[2]
[1] PhD Student, School of Engineering and Information Technology, UNSW Canberra, Australia
[2] Senior Lecturer, School of Engineering and Information Technology, UNSW Canberra, Australia
[4] mohammad.anwar-us-saadat@student.adfa.edu.au

Abstract: Stainless steel is a group of steel alloy with versatile crystal structures and material behaviours. Its characteristic nonlinear, rounded stress-strain behaviour without well-defined yield point makes it different from carbon steel. The degree of nonlinearity and roundness vary significantly from one grade of stainless steel to another which also increases the challenge to give a uniform formula for predicting the ultimate capacity of stainless steel sections of all grades. Presence of initial geometric imperfection and residual stress in structural member lead to premature yielding and loss of stiffness eventually reduces the load bearing capacity. For both structural design and finite element simulations, knowledge of their magnitude and distribution is therefore important. Recent years saw keen interest from the researchers on discovering the imperfection and residual stress pattern of stainless steel welded I-sections. Current study utilizes these findings to develop of finite element (FE) models for previously experimented stainless steel I-beams subjected to lateral-torsional buckling. Types of initial geometric imperfections, residual stresses and boundary conditions were varied in the FE models. Capacity of the developed FE models when compared with that of the lateral-torsional buckling experiments, revealed the influence of the variables considered. Understandings from this study will help further to develop finite element models for parametric study on stainless steel I-beams, consequently leading to evaluate the performance of the international design guidelines and propose new formulations.

1 Introduction

Stainless steel is gaining attention in current construction industry due to improved aesthetics, corrosion resistance, ductility and maintenance issues. In spite the behavioral difference between ordinary carbon steel and stainless steel in aspect of material properties, existing design codes initially adopted the design rules of carbon steel for designing stainless steel members. Unlike carbon steel stainless steel stress-strain curve is of rounded nature, with a high strain-hardening zone. Upon perceiving this difference in material behaviour, a new stainless steel design method was proposed which considers the strain-hardening and material nonlinearity of stainless steel (Gardner, 2002, Ashraf et al., 2008). This method produced better predictions when compared to international design guidelines. Consequent improvement were brought in to the design method, naming it as Continuous Strength Method (CSM), due to the fact the design method calculates the capacity of stainless steel section as a continuous function of the cross-section properties (Gardner et al., 2013, Afshan and Gardner, 2013, Ahmed et al., 2016). Development of CSM to become more useful as a design tool formulations were proposed to design cross-sections at individual and combined loading conditions (Liew and Gardner, 2015, Zhao et al., 2015, Anwar-Us-

Saadat et al., 2016). Initial works on member design were conducted on the flexural buckling of stainless steel welded I-section columns (Ahmed et al., 2015) and on the beam-column design of rectangular and square hollow section (RHS and SHS) columns. However, the design of lateral-torsional buckling (LTB) of stainless steel I-section beams using CSM is still to examine. This paper takes an initiative towards exploration of lateral-torsional buckling behaviour of stainless steel I-beams through numerical modelling of available experimental test results. Firstly, available test results concerning stainless steel and I-section beams subjected to lateral-torsional buckling were discussed. Later, principles of developing numerical finite element (FE) model were explained with an emphasis on inclusion of initial geometric imperfection and residual stress. Finally obtained FE results were compared with the test results to observe the effects of imperfections on the behaviour of stainless steel I-sections.

2 Test Programs on Lateral-torsional Buckling of Stainless steel I-sections

Though recently there have been a lot research and test programs conducted on stainless steel sections. Experimental programs on relating to lateral-torsional buckling are still rare. First attempt on this were made by van der Merwe et al. (1990). There, two cold-formed channels were back-to-back spot welded to manufacture of I-section. The channels were of 15 mm in flange dimension and 50 mm in web depth, thus making the width of I-section 30mm and depth 50mm. There were three different material types of stainless steel, austenitic 304 (EN 1.4301), ferritic 430 (EN 1.4016) and 3Cr12 (EN 1.4003). Total 8 specimens were test varying the length for each material type. Next effort was by Bredenkamp et al. (1996) on the hot rolled 3Cr12 chromium steel. There were 7 different beam lengths of one cross-section type which have been tested. Results from these studies were used to compare the performance of lateral-torsional buckling curves using tangent modulus approach and the curves for carbon steel adopted in then Canadian and South African hot-rolled steel design guidelines.

In the development of effective stainless steel design guideline in European aspect, experiments were performed on various types of stainless steel cross-sections (Burgan et al., 2000). Among these, tests on stainless steel welded I-sections were reported in a research report (ECSC, 2000). There were 12 specimens, 9 from austenitic (EN 1.4301) and 3 from duplex (EN 1.4462) which had been tested. Later finite element models of the test specimen were developed and results of the FE models were compared. These results were used to evaluate performance of the EN 1993-1-4 guidelines which was developed based on carbon steel design guideline of EN 1993-1-1. Recently, a lateral-torsional buckling experimental program was undertaken by (Wang et al., 2014), where total 10 welded stainless steel I-section beams of austenitic grade EN 1.4401 were tested. Among the tested specimens, 6 were equal flanged doubly symmetric sections, rest 4 were singly symmetric sections with width variations in compression and tension flange. In the following sections the test results from the last two experimental programs were utilized to develop FE models in order to check the effects of initial imperfection and residual stress.

3 Finite element modelling

It is not economically viable to conduct experiment for every aspect of a material or, specimen. In order to fill the gap of knowledge which can't be covered by experiments, finite element (FE) modelling techniques are widely used. In this study the test results were tried to mimic by the FE modelling using the commercial software (ABAQUS, 2014).

3.1 Basic Modelling Techniques

FE models were developed using S4R reduced integration shell elements, this element was successfully used by previous researchers (Ashraf et al., 2006, Theofanous and Gardner, 2009, Zhao et al., 2015, Anwar-Us-Saadat et al., 2016, Ahmed et al., 2016). Abaqus requires the material property to be provided as true stress vs. log plastic strain format in the property module. Stainless steel possess a nonlinear rounded stress-strain nature which was firstly described using equations provided by Ramberg and Osgood (1943), also popularly known as, *Ramberg-Osgood* material model. Gradually this was further

developed and modified to best fit with the exact material behaviour, thus currently different versions of modified *Ramberg-Osgood* equation exists (Mirambell and Real, 2000, Gardner and Ashraf, 2006, Quach et al., 2008). EN 1993-1-4 (2006) adopts the material model provided by Rasmussen (2003). This material model is based on the tension coupon test results and requires less number of parameters compared to other material models. Recently a thorough study (Arrayago et al., 2015) was conducted and the parameters concerning the Rasmussen (2003) material model was calibrated using a wide range of coupon test results. In the current study this material model was adopted using the tension coupon test results available from the test results.

3.2 Inclusion of Imperfections

Initial imperfection comes as an obvious property of the manufactured product, which often can have controlling effect on the member behaviour. Thus it is very important to consider within the FE models. Imperfections can be of two types, local and global. Local imperfection refers to the localized curving of the plates whereas global imperfection is related to the overall shape of member, also known as the bow imperfection. Common practice to include imperfection in to FE model is running a linear perturbation analysis prior to the nonlinear analysis, in order to derive the shape of the imperfection. Important is to decide that which type of imperfection will be significant for a member and correct amplitude of the imperfection.

Normal approach to derive the buckling shape is to load the member using similar method to be used in the nonlinear analysis. In order to obtain the moment capacity of a beam a four-point bending load system is used in the experiments (ECSC, 2000, Wang et al., 2014), as shown in Fig. 1. In this setup the unrestrained length between two load points receive a uniform moment. If this length is long, then the beam develop out of plane buckling shape with a torsional effect in the low eigenmode of a linear perturbation analysis. Local buckling shape can also be observed, but among the higher eigenmodes due to longer member length which is more prone to global buckling. For short length of beams the opposite is true, local shape occurs before the torsional buckling shape. When the effect of both imperfection types is require to study, finding the correct shape of two buckling modes from the eigenmode analysis becomes a dilemma, and time consuming task. Thus it is important to decide to what extent the members are sensitive to the effect of different type of imperfections. As a part of current research for all cases both local and global buckling shapes were used to develop FE models. Four amplitudes for the global imperfection were used (1) L/300, (2) L/500, (3) L/1000 and (4) L/1500 where, L is the unrestrained length between the load points of the beams. For local imperfection two separate value of imperfections were tested, (1) modified Dawson-Walker method (Gardner and Nethercot, 2004) as provided in Eqn. 1 and (2) $c_{flange}/200$, where, c_{flange} = (Flange width) /2 – (Web thickness) /2 – (Weld throat). In Eqn. 1, w_0 is the imperfection amplitude, $f_{0.2}$ is the 0.2% tensile proof stress, f_{cr} elastic critical buckling stress of the cross-section and t_{flange} is the flange thickness.

$$[1]\quad w_0 = 0.23 \times \frac{f_{0.2}}{f_{cr}} \times t_{flange}$$

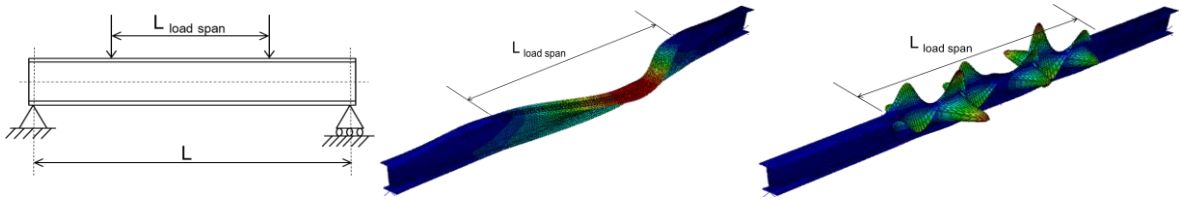

(a) (b) (c)

Figure 1: Buckling shape of beam in 4-point bending load system in a linear perturbation analysis, (a) load condition, (b) global buckling shape and (c) local buckling shape

3.3 Residual Stress due to welding

Similar to initial imperfection residual stresses exist in the members due to manufacturing process. More specifically, for a welded section residual stress arises from the welding process. Presence of residual stress might initiate loss of stiffening and premature yielding of the member, significantly reducing the carrying capacity of the member. Early experimental researches concerning residual stresses in welded I-section were conducted by Bredenkamp et al. (1992) and Lagerqvist and Olsson (2001). Later, these results were used by Gardner and Cruise (2009) and proposed a model to calculate residual stress in a welded stainless steel I-section. According to that study, membrane residual stresses are more significant than thorough thickness bending residual stress. Further comprehensive research was carried out by Yuan et al. (2014), where stainless steel welded box and I-sections were considered. They proposed new residual stress model for austenitic, duplex and ferritic grades of stainless steel. In the current research the FE models were modelled with and without residual stresses to observe the effect. The proposal given by Yuan et al. (2014) was used to incorporate the residual stresses in the model.

In order to apply the residual stress in the FE models, the cross-section was discretized in several blocks. Compressive and tensile residual stresses were applied using *INITIAL CONDITIONS command in ABAQUS (2014) in the relevant blocks. An additional step prior to the nonlinear step was added for allowing equilibrium due to the applied residual stress.

3.4 Boundary conditions and use of stiffeners in the FE model

In the test setup, simply supported boundary conditions are used for obtaining the beam strength (ECSC, 2000, Wang et al., 2014). During the FE modelling end sections of the FE models were tied with a reference point at bottom flange, where the translational movement about both cross-sectional axes were restricted. Longitudinal translation was restricted at one end and open at another to mimic the simply supported boundary condition. Rotation was allowed about the horizontal cross-section axis, whereas rotation about vertical cross-section axis and longitudinal axis were also restricted at the ends of the beam. During experiments at the loading points, stiffeners were used to increase the stiffness of the web. Thus, the cross-section around the loading point does not buckle due to localized effect of the load. Here FE models were developed in two methods one with stiffeners and another without stiffeners, in order to check the effect of stiffeners, deformation was applied in the top flange in the models with stiffeners. The stiffener was tied with the main I-section restricting inter-plate movement within them. The models without stiffeners had the whole cross-section at the loading point tied with a reference point at the top of the section and deformation was applied at that reference point. The boundary conditions imposed on the reference point was applicable for the whole cross-section at that point. Hence, when a vertical displacement was applied on the reference point, surrounding cross-section was also displaced vertically altogether, eradicating the risk of being locally displaced due to high concentration of load. Both types of FE models had there cross-sectional translation and rotation about vertical axis restricted to mimic the experimental boundary conditions. Now interesting would be to observe how these two kind of beams perform in comparison to each other.

4 Comparison of FE results with experiments

Firstly the FE models developed according to the test specimens where stiffeners are used in the loading locations were examined. These comparisons are provided in Table 1. For this occasion, various factors which might have effect on the capacity of the I-section beam, as initial geometric imperfections and residual stresses were compared. All FE models were included with residual stresses and combination of local and global buckling amplitudes. As described in the earlier section, 4 different types of global and 2 different local buckling amplitudes were used. Among the local buckling amplitudes, D-W refers to the amplitude obtained from modified Dawson-Walker model. Comparison with the test results were done using, the ratio of $M_{u,FE}/M_{u,Test}$. From Table 1 it can be observed, on the overall capacity of the members, local buckling amplitudes have less effects compared to global buckling. Best suited global buckling amplitude was L/300 producing average $M_{u,FE}/M_{u,Test}$ of 1.001 with coefficient of variance (CoV) 0.082.

In order to simplify the modelling process, the next modelling approach was to check performance of the FE models without stiffeners. As learnt in the previous paragraph, best results of FE models were obtained using global imperfection of L/300 amplitude, thus only this amplitude was utilized to develop the FE models without stiffeners. From Table 2 it can be seen that the FE models analysed without the stiffeners are also capable of producing quite accurate results, with average $M_{u,FE}/M_{u,Test}$ 1.013 with CoV 0.067. It can be concluded that, the process of model development can be simplified without using stiffeners as exact as the test setup, with the mentioned boundary conditions yet maintaining a decent level of accuracy.

Effect of residual stresses was investigated next using the FE models developed without stiffeners. Table 2 shows the comparison among the FE models developed with and without residual stresses. Results reveal models without residual stresses though produce quite accurate results still, less accurate to the models having residual stresses. Hence it can be understood that, residual stresses have definite capacity reduction effect on the ultimate moment of the test specimen analysed. In future models residual stresses will definitely be included in the FE models.

To determine the local buckling effect, full scale load and deformation curve were examined as can be seen in Fig. 2 and 3. Among the pool of validated test results two specimens were selected for this purpose. One EI-100-266-1 and another EI-100-266-5, here first one had higher member slenderness of 0.91 and another a bit lower 0.57 as the geometric properties provided in Wang et al. (2014). From the full load-deformation curves it can be seen that, the FE results were very close among themselves. A closure look in the following picture provides a better view to the comparison. In case of both member slendernesses it can be observed that the imperfection amplitude obtained from the Dawson-Walker model is much closure to the actual test response. Thus it can be used successfully to model the local buckling effects on the FE models for the parametric studies.

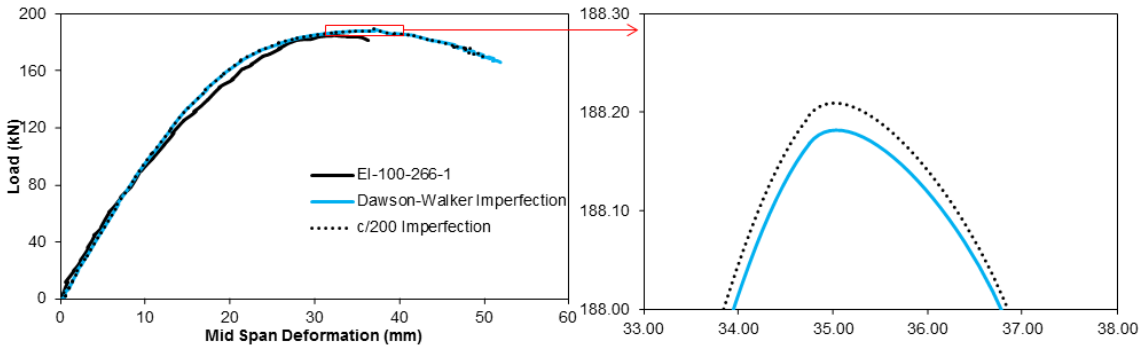

Figure: 2 Comparison between the overall load deformation curves of EI-100-266-1 to obtain the effect of local imperfection amplitude.

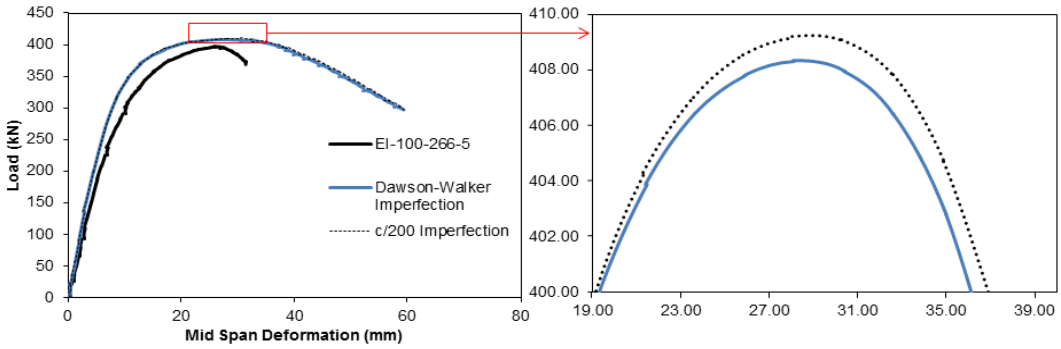

Figure: 3 Comparison between the overall load deformation curves of EI-100-266-5 to obtain the effect of local imperfection amplitude.

Table 1: Comparison of FE and experimental results using FE models using stiffeners

Source	Global buckling amplitude	$L_{load}/300$		$L_{load}/500$		$L_{load}/1000$		$L_{load}/1500$	
	Local buckling amplitude	D-W	c/200	D-W	c/200	D-W	c/200	D-W	c/200
	Test Specimen	$M_{u,FE}/M_{u,Test}$	$M_{u,FE}/M_{u,Test}$	$M_{u,FE}/M_{u,Test}$	$M_{u,FE}/M_{u,Test}$	$M_{u,FE}/M_{u,Test}$	$M_{u,FE}/M_{u,Test}$	$M_{u,FE}/M_{u,Test}$	$M_{u,FE}/M_{u,Test}$
Wang et al. (2014)	EI-100-266-1	0.986	0.985	0.997	0.997	1.059	1.060	1.072	1.073
	EI-100-266-2	0.891	0.892	0.926	0.926	0.949	0.950	0.960	0.961
	EI-100-266-3	0.938	0.938	0.970	0.971	0.990	0.991	1.001	1.001
	EI-100-266-4	1.051	1.050	1.073	1.073	1.089	1.088	1.096	1.096
	EI-100-266-5	0.994	0.995	1.015	1.016	1.028	1.030	1.033	1.037
	EI-100-266-6	1.020	1.022	1.038	1.039	1.049	1.051	1.054	1.057
ECSC (2000)	I-160x80-B0	0.951	0.951	0.964	0.964	0.972	0.972	0.976	0.976
	I-160x80-B1	1.036	1.036	1.050	1.050	1.059	1.059	1.063	1.064
	I-160x80-B2	1.022	1.021	1.038	1.037	1.075	1.076	1.093	1.094
	I-160x160-B0	0.870	0.851	0.898	0.866	0.923	0.875	0.936	0.878
	I-160x160-B1	0.985	0.985	0.995	0.995	1.026	1.026	1.049	1.049
	I-160x160-B2	1.131	1.131	1.140	1.140	1.188	1.187	1.210	1.210
	I-160x160-DUPLEX-B0	0.886	0.902	0.915	0.966	0.942	0.946	0.960	0.933
	I-160x160-DUPLEX-B1	1.155	1.154	1.157	1.157	1.159	1.159	1.160	1.160
	I-160x160-DUPLEX-B2	0.964	0.964	0.972	0.972	1.018	1.018	1.039	1.039
	I-320x160-B0	0.943	0.948	0.961	0.970	0.977	0.987	0.982	0.987
	I-320x160-B1	1.061	1.063	1.077	1.080	1.091	1.093	1.097	1.098
	I-320x160-B2	1.133	1.132	1.152	1.151	1.198	1.200	1.218	1.220
	Average	1.001	1.001	1.019	1.021	1.044	1.043	1.056	1.052
	CoV	0.082	0.082	0.075	0.075	0.075	0.079	0.075	0.083

Table 2: Comparison among FE models with and without residual stresses

Source	Test Specimen	With residual stress		Without residual stress	
		$M_{u,FE}/M_{u,Test}$	$M_{u,FE}/M_{u,Test}$	$M_{u,FE}/M_{u,Test}$	$M_{u,FE}/M_{u,Test}$
Wang et. al. (2014)	EI-100-266-1	1.022	1.022	1.047	1.047
	EI-100-266-2	0.918	0.917	0.935	0.935
	EI-100-266-3	0.957	0.958	0.972	0.971
	EI-100-266-4	1.049	1.049	1.057	1.058
	EI-100-266-5	1.011	1.013	1.014	1.015
	EI-100-266-6	1.031	1.028	1.034	1.031
ECSC (2000)	I-160x80-B0	0.959	0.958	0.960	0.959
	I-160x80-B1	1.043	1.043	1.045	1.044
	I-160x80-B2	1.028	1.028	1.051	1.051
	I-160x160-B0	0.922	0.922	0.922	0.922
	I-160x160-B1	1.062	1.062	1.085	1.086
	I-160x160-B2	1.142	1.142	1.176	1.176
	I-160x160-DUPLEX-B0	0.956	0.955	0.954	0.954
	I-160x160-DUPLEX-B1	1.041	1.041	1.044	1.044
	I-160x160-DUPLEX-B2	0.976	0.976	1.048	1.048
	I-320x160-B0	0.905	0.905	0.911	0.911
	I-320x160-B1	1.057	1.053	1.060	1.056
	I-320x160-B2	1.151	1.151	1.199	1.199
	Average	1.013	1.012	1.028	1.028
	CoV	0.067	0.067	0.074	0.074

5 Conclusion

A thorough investigation on the effects of initial imperfection and residual stresses on the lateral torsional moment capacity were performed using numerical FE modelling. FE models of total 18 test results were generated using various conditions of boundary conditions, imperfection amplitudes and residual stresses. Comparison among the test results and FE models using stiffeners and without stiffeners show that effect of stiffeners can mitigated if an appropriate boundary condition is utilized. Thus for parametric studies in future the FE models will be developed without stiffeners. Among two types of initial geometric imperfections, global imperfection has more effect on the capacity compared to the local imperfection. Global imperfection amplitudes calculated as a factor of 1/300 multiplied with the unrestrained length of load span founded to be the most effective one. Local buckling imperfection amplitudes used produce very close results on the FE models capacity prediction. Inspection of the load-deformation behaviour reveals, amplitude produced from modified Dawson-Walker model produces somewhat more accurate representation of the behaviour. Residual stress formulations from Yuan et al. (2014) yielded exact model behaviour in comparison with the test results. However, effect of residual stresses is important to the ultimate capacity as seen from the FE models analysed without residual stresses. This study provides a basis of developing the numerical FE models for stainless steel welded I-section beams at lateral torsional buckling. Extracts from this study will be further utilized to develop parametric FE models and proposing newer formulations on LTB of stainless steel I-beams.

6 References

ABAQUS. 2014. *ABAQUS Version 6.14, user documentation* [Online]. Providence, RI: Dassault Systemes.

Afshan, S. & Gardner, L. 2013. The continuous strength method for structural stainless steel design. *Thin-Walled Structures,* 68**,** 42-49.

Ahmed, S., Ashraf, M. & Al-Deen, S. Empirical formulations for predicting the flexural buckling resistance of stainless steel columns. *In:* CAMOTIM, D., ed. Eigth International Conference of Advances on Steel Structures (ICASS 2015), 2015 Lisbon, Portugal.

Ahmed, S., Ashraf, M. & Anwar-Us-Saadat, M. 2016. The Continuous Strength Method for slender stainless steel cross-sections. *Thin-Walled Structures,* 107**,** 362-376.

Anwar-Us-Saadat, M., Ashraf, M. & Ahmed, S. 2016. Behaviour and design of stainless steel slender cross-sections subjected to combined loading. *Thin-Walled Structures,* 104**,** 225-237.

Arrayago, I., Real, E. & Gardner, L. 2015. Description of stress–strain curves for stainless steel alloys. *Materials & Design,* 87**,** 540-552.

Ashraf, M., Gardner, L. & Nethercot, D. A. 2006. Finite element modelling of structural stainless steel cross-sections. *Thin-Walled Structures,* 44**,** 1048-1062.

Ashraf, M., Gardner, L. & Nethercot, D. A. 2008. Structural stainless steel design: Resistance based on deformation capacity. *Journal of structural engineering,* 134**,** 402-411.

Bredenkamp, P., Barnard, H., Van den Berg, G. & Van der Merwe, P. 1996. The lateral-torsional buckling strength of hot-rolled stainless steel beams. *STRUCTURAL ENGINEER,* 74**,** 316-318.

Bredenkamp, P., Van den Berg, G. & Van der Merwe, P. 1992. Residual stresses and the strength of stainless steel I-section columns. *Proc., Structural Stability Research Council***,** 69-86.

Burgan, B., Baddoo, N. & Gilsenan, K. 2000. Structural design of stainless steel members—comparison between Eurocode 3, Part 1.4 and test results. *Journal of Constructional Steel Research,* 54**,** 51-73.

ECSC 2000. Work Packages 3.1, 3.2 and 3.3 Beams, Columns and Beam-columns Welded I-Sections. *In:* STANGENBERG, H. (ed.) *Development of the use of stainless steel in construction.* Finland: RWTH and VTT.

EN 1993-1-4 2006. Eurocode 3: Design of steel structures – Part 1.4:General rules – supplementary rules for stainless steels. Brussels: European Committee for Standardization (CEN).

Gardner, L. 2002. *A new approach to structural stainless steel design.* PhD PhD Thesis, Imperial College of London.

Gardner, L. & Ashraf, M. 2006. Structural design for non-linear metallic materials. *Engineering Structures,* 28**,** 926-934.

Gardner, L. & Cruise, R. 2009. Modeling of residual stresses in structural stainless steel sections. *Journal of Structural Engineering,* 135**,** 42-53.

Gardner, L., Kucukler, M. & Macorini, L. 2013. The continuous strength method for steel and composite design. *Proceedings of the ICE - Structures and Buildings,* 166**,** 434-443.

Gardner, L. & Nethercot, D. 2004. Numerical modeling of stainless steel structural components-A consistent approach. *Journal of Structural Engineering,* 130**,** 1586-1601.

Lagerqvist, O. & Olsson, A. Residual stresses in welded I-girders made of stainless steel and structural steel. 9th Nordic Steel Construction Conference, 18/06/2001-20/06/2001 2001 Helsinki, Finland. Helsinki University of Technology.

Liew, A. & Gardner, L. Ultimate capacity of structural steel cross-sections under compression, bending and combined loading. Structures, 2015. Elsevier, 2-11.

Mirambell, E. & Real, E. 2000. On the calculation of deflections in structural stainless steel beams: an experimental and numerical investigation. *Journal of Constructional Steel Research,* 54**,** 109-133.

Quach, W., Teng, J. & Chung, K. 2008. Three-Stage Full-Range Stress-Strain Model for Stainless Steels. *Journal of Structural Engineering,* 134**,** 1518-1527.

Ramberg, W. & Osgood, W. R. 1943. *Description of stress-strain curves by three parameters, Technical Note no. 902,* Washington DC, National advisory committee for aeronautics.

Rasmussen, K. J. R. 2003. Full-range stress–strain curves for stainless steel alloys. *Journal of Constructional Steel Research,* 59**,** 47-61.

Theofanous, M. & Gardner, L. 2009. Testing and numerical modelling of lean duplex stainless steel hollow section columns. *Engineering Structures,* 31**,** 3047-3058.

van der Merwe, P., Van Wyk, M. & van den Berg, G. Lateral torsional buckling strength of doubly symmetric stainless steel beams. *In:* YU, W.-W. & LABOUBE, R. A., eds. International Specialty Conference on Cold-Formed Steel Structures, October 23-24, 1990 1990 St. Louis, Missouri. Department of Civil Engineering University of Missouri - Rolla.

Wang, Y., Yang, L., Gao, B., Shi, Y. & Yuan, H. 2014. Experimental study of lateral-torsional buckling behavior of stainless steel welded I-section beams. *International Journal of Steel Structures,* 14**,** 411-420.

Yuan, H. X., Wang, Y. Q., Shi, Y. J. & Gardner, L. 2014. Residual stress distributions in welded stainless steel sections. *Thin-Walled Structures,* 79**,** 38-51.

Zhao, O., Rossi, B., Gardner, L. & Young, B. 2015. Behaviour of structural stainless steel cross-sections under combined loading–Part II: Numerical modelling and design approach. *Engineering Structures,* 89**,** 247-259.